International Journal of Engineering Science 62 (2013) 157–164

Contents lists available at SciVerse ScienceDirect

International Journal of Engineering Science

journal homepage: www.elsevier.com/locate/ijengsci

Short Communication

Inducing compressive residual stress in microscale print-lines for flexible electronics

T.I. Zohdi

Department of Mechanical Engineering, 6195 Etcheverry Hall, University of California, Berkeley, CA 94720-1740, USA

ARTICLE INFO

Article history:
Received in revised form 24 September 2012
Accepted 25 September 2012
Available online 7 November 2012

Keywords:
Electronics
Print-lines
Thermal shrinkage
Damage

ABSTRACT

Printed electronics are becoming widespread in modern industrial devices. In many of the manufacturing processes of printed electronics, one step is the deposition of initially molten (or liquid), microscale, "print-lines" of material onto a flexible substrate. As the deposited molten print-line solidifies, the bonded print-line and substrate may have the tendency to curl (attain a finite curvature), due to the differences in the thermal expansion coefficients, elastic properties, etc. The quality and durability of the solidified print-line (which is mechanically-weak) is adversely affected by residual tensile stress states. Tensile stress states have a tendency to induce damage in the form of cavities or cracks in the deposited material, which would hinder the printed electronics operation. Therefore, ideally, one would like the solidified print-line to be in a state of compression. Inducing a compressive stress-state in the print-line is particularly important in the vicinity of the substrate interface, since damage in that location may also initiate delamination of the deposited material and, eventually, a malfunction of the intended printed electronics application. In this work, employing an elementary thermo-mechanical model, a mathematical expression is derived for the combination of system parameters needed to ensure that the print-line material at remains in a compressive state at the bimaterial interface.

1. Introduction

The motivation for this work is the large increase in the use of print-based manufacturing. In particular, printed electronics on flexible foundational substrates are becoming popular, and have a wide-range of applications, such as flexible solar cells and smart electronics. One important technological obstacle is to develop inexpensive, durable electronic material-units that reside on flexible platforms/substrates which can be easily deployed onto large surface areas. Print-based methods are, in theory, ideal for large-scale applications, and provide a framework for assembling electronic circuits by mounting printed electronic devices on flexible plastic substrates, such as polyimide and "PEEK" (Poly-Ether–Ether–Ketone, a flexible thermoplastic polymer) film. There are many variants of this type of technology, which is sometimes referred to as flexible electronics or flex circuits. Flex circuits can be, for example, screen printed silver circuits on polyester. For an early history of the printed electronics field (see Gamota, Brazis, Kalyanasundaram, & Zhang, 2004).

Regardless of the exact method of print-line deposition, the common physics is a curing bimaterial system of disparate properties. The objective of this paper is to provide a design criteria to achieve high-quality print-lines (Fig. 1). One important criteria for a high-quality print-line is that the initially molten (or liquid) deposited print-line material be in compression when the system cures/cools. The reasoning for this is that a compressive state is much more resistant to damage than a

E-mail address: zohdi@newton.berkeley.edu

0020-7225/$ - see front matter © 2012 Elsevier Ltd. All rights reserved.
http://dx.doi.org/10.1016/j.ijengsci.2012.09.004

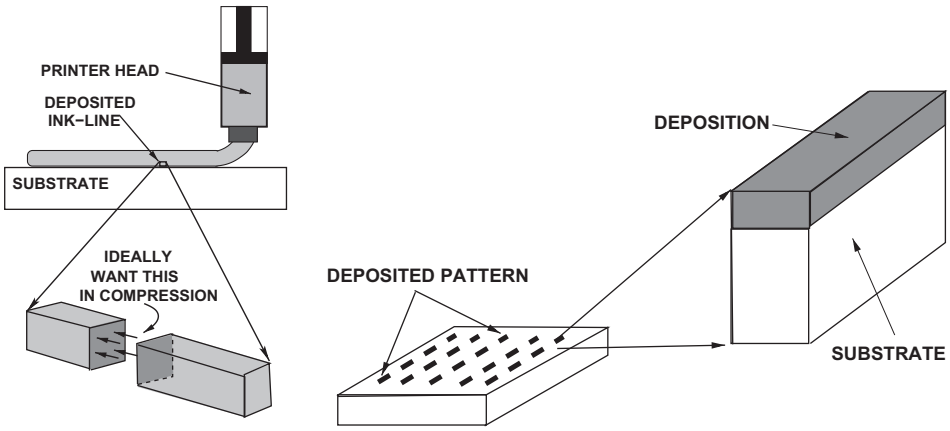

Fig. 1. Left: deposited print-line. Right: an extracted section of a printed pattern-a thermally-cooling deposition on a piece of substrate (both are assumed flexible/compliant).

tensile state. Attaining a compressive stress-state in the print-line is critical in the vicinity of the bimaterial interface, since the damage in that location may also initiate delamination of the deposited material and, ultimately, a complete breakdown of the printed electronics application. In this paper, we focus on isolated print-line deposited on a strip (coupon) of substrate material. The overall idealized process that we analyze is as follows, using a simple one-dimensional stress-state ("strength-of-materials") model for each strip:

- The "hot" material (print-line/substrate) are bonded together, and are initially of equal length.
- The materials are cooled by $\Delta\theta = \theta - \theta_0$.
- The interface remains perfectly bonded.
- The system is in static equilibrium.
- The temperature of the system is uniform.

Remark 1. In order to develop flexible micro/nanoelectronics for large area deployment, traditional methods of fabrication using silicon-based approaches have become limited for applications that involve large-area coverage, due to high cost of materials and equipment (which frequently need a vacuum environment). For flexibility and lower cost, the ability to develop these electronics on plastics is necessary. To accomplish this task, print-based technologies are starting to become popular for these applications. In many cases, this requires the development of nanoparticle-functionalized "inks". These nanoparticles include germanium (which has higher mobility and better tailorable absorption spectrum for ambient light than silicon) and silver (which is being studied due to the possibility to sinter the particles even without the need of directly applied intense heating). Other semiconductor nanoparticles, including zinc and cadmium based compounds and metals, such as gold and copper, can be considered. Precise patterning of (nanoparticle-functionalized) prints is critical for a number of different applications. For example, some recent applications include low temperature electrode deposition (Huang, Liao, Molesa, Redinger, & Subramanian, 2003) optical coatings and photonics (Maier & Atwater, 2005; Nakanishi et al., 2009) biosensors (Alivisatos, 2004), catalysts (Haruta, 2002) and MEMS applications (Fuller, Wilhelm, & Jacobson, 2002; Ho et al., 2006). Several methods are available for patterning nanoparticles, the most popular of which is inkjet printing (Ridley, Nivi, & Jacobson, 1999; Sirringhaus et al., 2000). Inkjet printing is attractive due to its simplicity, high throughput, and low material loss. However, patterning with inkjet printing is limited to a resolution of around 20–50 μm with current printers (Ridley et al., 1999) with higher resolution possible by adding complexity to the substrate prior to printing (Wang, Zheng, Li, Huck, & Sirringhaus, 2004). Electrohydrodynamic printing has also been proposed to increase the resolution beyond the limits of inkjet printing, achieving a line resolution as small as 700 nm (Park et al., 2007). Due to the nature of the deposited materials, they are adversely affected by tensile stress states when they solidify.

2. An idealized purely extensional deformation

In order to initially illustrate some simple concepts, consider a simplified first problem, comprised of a system of two bonded layers, with *no induced curvature (bending)*. We assume:

- The strips are bonded together, initially at the same temperature and all the same length.
- The strips are cooled down simultaneously.
- The strips have different stiffnesses and thermal expansion coefficients than the inner layer.

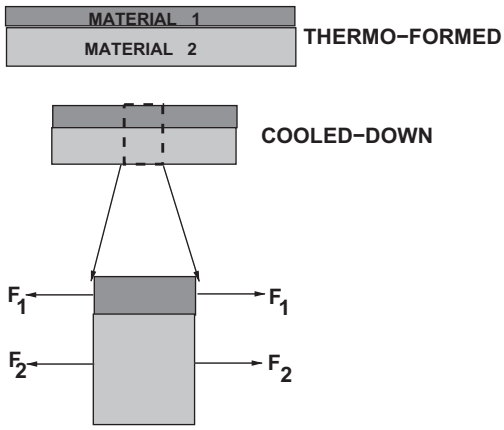

Fig. 2. An illustrative first problem: a system of bonded strips with an idealization of no thermally-induced curvature changes.

Referring to Fig. 2, there are two contributions to the strain. The strain due to the extensional load in material 1 is

$$\epsilon_1^e = \frac{F_1}{E_1 A_1} \tag{1}$$

and in material 2 is

$$\epsilon_2^e = \frac{F_2}{E_2 A_2}. \tag{2}$$

The thermal contribution in material 1 is

$$\epsilon_1^\theta = \alpha_1 \Delta\theta \tag{3}$$

and in material 2 is

$$\epsilon_2^\theta = \alpha_2 \Delta\theta. \tag{4}$$

For perfectly bonded one-dimensional strip kinematics, one equates the total normal strain in both materials to give

$$\epsilon_1^e + \epsilon_1^\theta = \epsilon_2^e + \epsilon_2^\theta, \tag{5}$$

which implies

$$\frac{F_1}{E_1 A_1} + \alpha_1 \Delta\theta = \frac{F_2}{E_2 A_2} + \alpha_2 \Delta\theta. \tag{6}$$

Since the system is in static equilibrium, we must also have that the sum of the forces is zero

$$\sum F = F_1 + F_2 = 0. \tag{7}$$

Solving Eqs. (6) and (7) simultaneously for the force in material 1 yields:

$$F_1 = \frac{(\alpha_2 - \alpha_1)\Delta\theta}{\kappa} \tag{8}$$

and for the force in material 2:

$$F_2 = -\frac{(\alpha_2 - \alpha_1)\Delta\theta}{\kappa}, \tag{9}$$

where

$$\kappa \stackrel{\text{def}}{=} \frac{1}{E_1 A_1} + \frac{1}{E_2 A_2}. \tag{10}$$

The total strain in material 1 is

$$\epsilon_1^{tot} = \frac{(\alpha_2 - \alpha_1)\Delta\theta}{E_1 A_1 \kappa} + \alpha_1 \Delta\theta \tag{11}$$

and for material 2 is

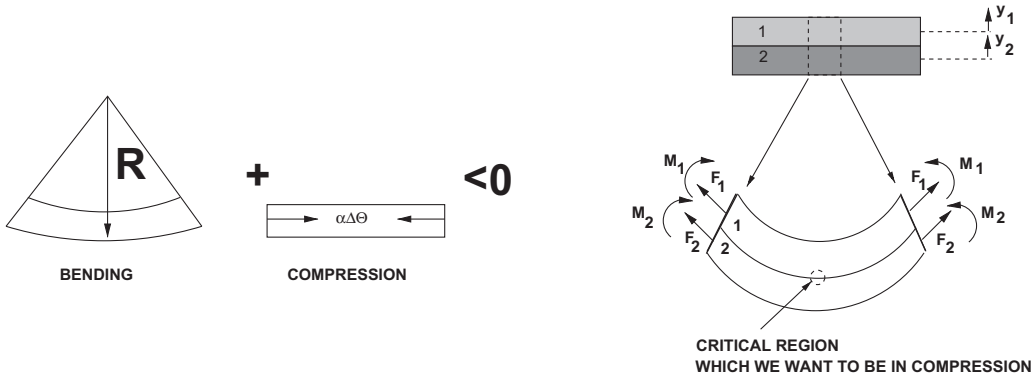

Fig. 3. Left: pictorial representation of a combined thermally-induced bending and extensional effects that must be controlled. Right: a curling system of bonded strips.

$$\epsilon_2^{tot} = -\frac{(\alpha_2 - \alpha_1)\Delta\theta}{E_2 A_2 \kappa} + \alpha_2 \Delta\theta. \tag{12}$$

In order to attain the condition that material 1 be in compression at the interface, we must have[1]

$$\sigma_1 = E_1\left(\epsilon_1^{tot} - \alpha_1\Delta\theta\right) \leqslant 0 \Rightarrow \epsilon_1^{tot} \leqslant \alpha_1\Delta\theta \Rightarrow \frac{(\alpha_2 - \alpha_1)\Delta\theta}{E_1 A_1 \kappa} \leqslant 0, \tag{13}$$

which arises from using Eq. (11). If $\Delta\theta \leqslant 0$, then

$$\frac{(\alpha_2 - \alpha_1)\Delta\theta}{E_1 A_1 \kappa} \geqslant 0. \tag{14}$$

Thus, for a compressive state to be induced, we must have $\alpha_2 \geqslant \alpha_1$. Clearly, this is intuitive, since if the substrate contracts more it will compress (pull inwards) the outer layers. Next, we consider the more complex case which includes curvature changes and hence bending stresses.

3. Combined thermal, extensional and bending deformation

Referring to Fig. 3, there are three contributions to the strain. The strain, due to the extensional load in material 1, is

$$\epsilon_1^e = \frac{F_1}{E_1 A_1} \tag{15}$$

and in material 2

$$\epsilon_2^e = \frac{F_2}{E_2 A_2}. \tag{16}$$

The strain, due to bending (curvature changes), in material 1 is

$$\epsilon_1^b = -\frac{M_1 y_1}{E_1 I_1} \tag{17}$$

and in material 2 is

$$\epsilon_2^b = -\frac{M_2 y_2}{E_2 I_2}. \tag{18}$$

The thermal contraction contribution for material 1 is

$$\epsilon_1^\theta = \alpha_1 \Delta\theta \tag{19}$$

and for material 2 is

$$\epsilon_2^\theta = \alpha_2 \Delta\theta. \tag{20}$$

For this simple model, at the perfectly bonded interface, one equates the total normal strain at the interface to yield

[1] In the present case, where there is no bending, the layer has a uniform stress with the one-dimensional strength-of-materials solution.

$$\epsilon_1^e + \epsilon_1^b + \epsilon_1^\theta = \epsilon_2^e + \epsilon_2^b + \epsilon_2^\theta, \tag{21}$$

which gives, at $y_1 = y_1^{int}$ and $y_2 = y_2^{int}$,

$$\frac{F_1}{E_1 A_1} - \frac{M_1 y_1^{int}}{E_1 I_1} + \alpha_1 \Delta\theta = \frac{F_2}{E_2 A_2} - \frac{M_2 y_2^{int}}{E_2 I_2} + \alpha_2 \Delta\theta. \tag{22}$$

Also, the curvatures of the strips must be equal

$$\frac{1}{R_1} = \frac{M_1}{E_1 I_1} = \frac{1}{R_2} = \frac{M_2}{E_2 I_2} \Rightarrow M_1 = M_2 \frac{E_1 I_1}{E_2 I_2}. \tag{23}$$

At a cross-section, statics dictates that the sum of the moments is zero (here, with summation about the interface)

$$\sum M = M_1 + M_2 - F_1 d_1^{int} + F_2 d_2^{int} = 0, \tag{24}$$

where $d_1^{int} = |y_1^{int}|$ is the distance from the neutral axis of material 1 to the interface, and $d_2^{int} = |y_2^{int}|$ is the distance from the neutral axis of material 2 to the interface. We must also have that the sum of the forces is zero

$$\sum F = F_1 + F_2 = 0. \tag{25}$$

Solving Eqs. (22)–(25) simultaneously for the 4 unknowns, F_1, F_2, M_1 and M_2 yields:

- For the force in material 1:

$$F_1 = \frac{(\alpha_2 - \alpha_1)\Delta\theta}{\Psi\Lambda}. \tag{26}$$

- For the force in material 2:

$$F_2 = -\frac{(\alpha_2 - \alpha_1)\Delta\theta}{\Psi\Lambda}. \tag{27}$$

- For the moment in material 1:

$$M_1 = \frac{(\alpha_2 - \alpha_1)\Delta\theta}{\Psi} \frac{E_1 I_1}{E_2 I_2}. \tag{28}$$

- For the moment in material 2:

$$M_2 = \frac{(\alpha_2 - \alpha_1)\Delta\theta}{\Psi}, \tag{29}$$

where

$$\Lambda = \frac{d_1^{int} + d_2^{int}}{\left(1 + \frac{E_1 I_1}{E_2 I_2}\right)} \tag{30}$$

and

$$\Psi = \frac{1}{\Lambda E_1 A_1} + \frac{d_1^{int}}{E_1 I_1} + \frac{1}{\Lambda E_2 A_2} + \frac{d_2^{int}}{E_2 I_2}. \tag{31}$$

The total strain anywhere in material 1 is

$$\epsilon_1^{tot} = \left(\frac{(\alpha_2 - \alpha_1)}{E_1 A_1 \Psi \Lambda} - \frac{(\alpha_2 - \alpha_1)}{\Psi} \frac{y_1}{E_2 I_2} + \alpha_1\right)\Delta\theta \stackrel{\text{def}}{=} \gamma_1 \Delta\theta \tag{32}$$

and the total strain anywhere in material 2 is

$$\epsilon_2^{tot} = -\left(\frac{(\alpha_2 - \alpha_1)}{E_2 A_2 \Psi \Lambda} + \frac{(\alpha_2 - \alpha_1)}{\Psi} \frac{y_2}{E_2 I_2} + \alpha_2\right)\Delta\theta \stackrel{\text{def}}{=} \gamma_2 \Delta\theta. \tag{33}$$

To meet the criteria that material 1 be in compression at the interface, we must have

$$\sigma_1 = E_1\left(\epsilon_1^{tot} - \alpha_1 \Delta\theta\right) \leqslant 0 \Rightarrow \epsilon_1^{tot} \leqslant \alpha_1 \Delta\theta \Rightarrow \gamma_1 \Delta\theta \leqslant \alpha_1 \Delta\theta. \tag{34}$$

If $\Delta\theta \leqslant 0$, then

$$\gamma_1 \Delta\theta \leqslant \alpha_1 \Delta\theta \Rightarrow \gamma_1 \geqslant \alpha_1, \tag{35}$$

which collapses, in the case of $\alpha_2 \geqslant \alpha_1$, to $\left(y_1^{int} = -d_1^{int}\right)$

$$\frac{\Lambda E_1 A_1 y_1^{int}}{E_2 I_2} \leqslant 1 \tag{36}$$

and in the case of $\alpha_2 \leqslant \alpha_1$, to

$$\frac{\Lambda E_1 A_1 y_1^{int}}{E_2 I_2} \geqslant 1. \tag{37}$$

4. Special cases and inverse problems

If we consider rectangular cross-sectional areas of the form $A_1 = b_1 h_1$ and $A_2 = b_2 h_2$, then $I_1 = \frac{1}{12} b_1 h_1^3$, $I_2 = \frac{1}{12} b_2 h_2^3$, $y_1^{int} = -d_1^{int} = -\frac{h_1}{2}$ and $y_2^{int} = d_2^{int} = \frac{h_2}{2}$, and substituting into Eq. (35), we have, in the case of $\alpha_2 \geqslant \alpha_1$

$$\frac{3\left(1 + \frac{h_2}{h_1}\right)}{\left(1 + \frac{E_2}{E_1}\frac{b_2 h_2^3}{b_1 h_1^3}\right)} \geqslant 1 \tag{38}$$

and in the case of $\alpha_2 \leqslant \alpha_1$

$$\frac{3\left(1 + \frac{h_2}{h_1}\right)}{\left(1 + \frac{E_2}{E_1}\frac{b_2 h_2^3}{b_1 h_1^3}\right)} \leqslant 1. \tag{39}$$

Thus, the material designer has a total eight free parameters for system with rectangular cross-sections, namely, four material parameters $(\alpha_1, \alpha_2, E_1, E_2)$ and four geometrical parameters (h_1, h_2, b_1, b_2). In cases where it is unlikely that one can find a set of parameters that satisfy case where Eq. (38) or (39) are valid, one consider attempt to minimize the amount of violation by considering the following cost function (regardless of whether $\alpha_1 > \alpha_2$, or vice versa) that represents attaining a zero stress state at the interface for material 1

$$\Pi(E_1, E_2, h_1, h_2, b_1, b_2) \stackrel{\text{def}}{=} \left(\frac{3\left(1 + \frac{h_2}{h_1}\right)}{\left(1 + \frac{E_2}{E_1}\frac{b_2 h_2^3}{b_1 h_1^3}\right)} - 1\right)^2. \tag{40}$$

A plot of Π is shown in Fig. 4. This allows one to determine appropriate combinations of the height of the deposition, thickness of the substrate and the thermo-elastic combinations of the substrate for a (neutral) zero-stress condition. Plots for parameter combinations which deliver compressive stress states can also be generated by adjusting the constant "1" on the righthand side of Eq. (38) or (39) with another appropriate constant.

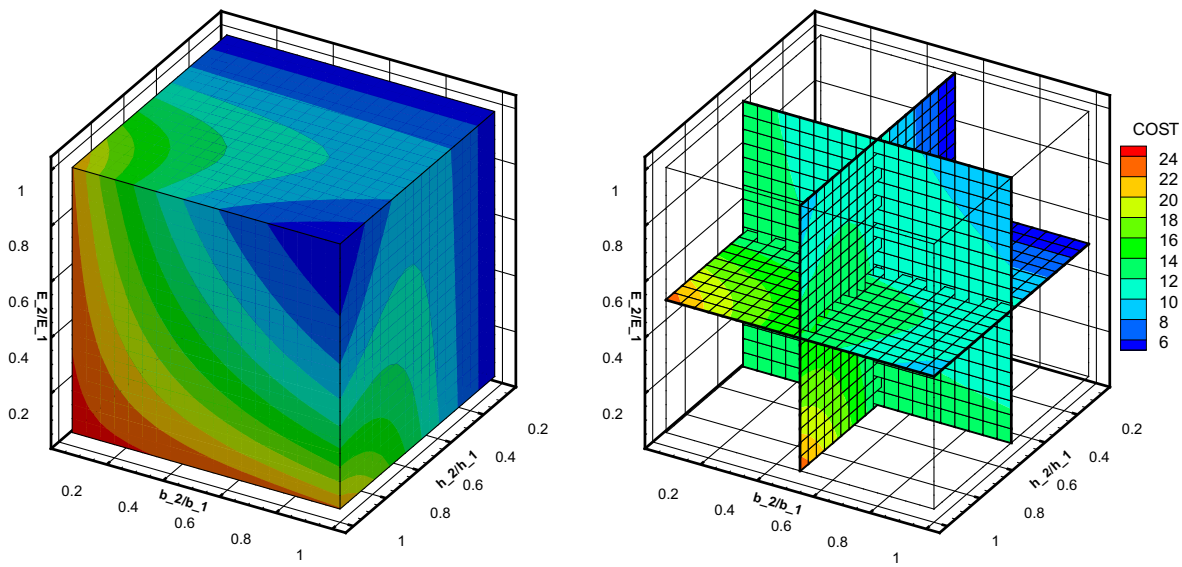

Fig. 4. Left: the full nondimensional parameter space for the values of Π. Right: orthogonal slices through parameter space. Clearly, blue regions are advantageous and red regions are not. (For interpretation of the references to color in this figure legend, the reader is referred to the web version of this article.)

Remark 1. One could apply Newton's method, by forming the Hessian and Gradient, and set up the following system of equations

$$\begin{bmatrix} \frac{\partial^2 \Pi}{\partial E_1^2} & \frac{\partial^2 \Pi}{\partial E_1 \partial E_2} & \cdots \\ \frac{\partial^2 \Pi}{\partial E_2 \partial E_1} & \frac{\partial^2 \Pi}{\partial E_2^2} & \cdots \\ \cdots & \cdots & \cdots \end{bmatrix} \begin{bmatrix} \left(E_1^{i+1} - E_1^i\right) \\ \left(E_2^{i+1} - E_2^i\right) \\ \cdots \end{bmatrix} = - \begin{bmatrix} \frac{\partial \Pi}{\partial E_1} \\ \frac{\partial \Pi}{\partial E_2} \\ \cdots \end{bmatrix} \tag{41}$$

However, because the system may not necessarily have unique minima (Π is nonconvex), the Hessian may not be positive definite, and thus nonconvex optimization techniques, may need to be used.

Remark 2. In the simplest case, where $h_1 = h_2$ and $b_1 = b_2$, in the case of $\alpha_2 \geqslant \alpha_1$, the criteria in Eq. (38) collapses to

$$E_2 \leqslant 5E_1 \tag{42}$$

and in the case of $\alpha_2 \leqslant \alpha_1$, the criteria in Eq. (38) collapses to

$$E_2 \geqslant 5E_1. \tag{43}$$

Specifically, the substrate must be at least five times stiffer than the print-line to retain a compressive state.

5. Summary

The simple analysis presented provides some general guidance on the material combinations that are the best choice to attain a compressive residual stress state. On a two dimensional surface, the criteria (if it even exists) is unclear, and is under investigation by the author. However, we note that a preliminary finite element analysis indicates that the nonconvex shapes of deposited films on substrates will be impossible to keep in compression throughout the curing film structure, due to the highly nonuniform states of stress. Finally, following up on the introductory comments on the type of technology that drives this analysis, we remark that, unfortunately, inkjet and electrohydrodynamic printing do not allow precise control over the structure of the printed lines. This often results in lines with scalloped edges or non-uniform widths, and offer only limited control over the height of the printed features (Ahmad, Rasekh, & Edirisinghe, 2010; Huang et al., 2003; Samarasinghe, Pastoriza-Santos, Edirisinghe, Reece, & Liz-Marzan, 2006; Sirringhaus et al., 2000). Recently, nanoimprint lithography has been proposed as a means of decreasing the feature size of patterned nanoparticles while allowing more precise control over the structure of the printed lines (Ko et al., 2007, 2008; Park et al., 2008). In this fabrication method, the nanoparticle inks are patterned by pressing with an elastomer mold and the particles are dried into their final configuration. While the resolution of nanoimprint lithography is an improvement over inkjet printing, there exists a residual layer on the substrate that must be etched away after patterning. Control over the height of features can be corrupted by capillary action between the mold and the drying ink, in particular along the length of longer features. Thus, as a possible alternative to nanoimprint lithography, nanoparticle self-assembly methods, based on capillary filling of photoresist templates have been proposed (Demko, Cheng, & Pisano, 2010), and appear to be promising. It is important to note that many of the processes involve evaporative cooling, and require a simultaneous heat and mass transfer analysis. A complete model and numerical simulation of this process is currently underway by the author.

Acknowledgments

The author expresses his gratitude to Mr. Gary Merrill, Ms. Cora Schillig and Dr. Ramesh Subramanian of the Siemens corporation for support of this research.

References

Ahmad, Z., Rasekh, M., & Edirisinghe, M. (2010). Electrohydrodynamic direct writing of biomedical polymers and composites. *Macromolecular Materials and Engineering, 295*, 315–319.

Alivisatos, P. (2004). The use of nanocrystals in biological detection. *Nature Biotechnology* (1), 47–52.

Demko, M. T., Cheng, J. C., & Pisano, A. P. (2010). High-resolution direct patterning of gold nanoparticles by the microfluidic molding process. *Langmuir*, 412–417.

Fuller, S. B., Wilhelm, E. J., & Jacobson, J. M. (2002). Ink-jet printed nanoparticle microelectromechanical systems. *Journal of Microelectromechanical Systems, 11*, 54–60.

Gamota, D., Brazis, P., Kalyanasundaram, K., & Zhang, J. (2004). *Printed organic and molecular electronics*. New York: Kluwer Academic Publishers.

Haruta, M. (2002). Catalysis of gold nanoparticles deposited on metal oxides. *Cattech, 6*(3), 102–115.

Ho, C., Steingart, D., Salminent, J., Sin, W., Rantala, T., Evans, J., & Wright, P. (2006). Dispenser printed electrochemical capacitors for power management of millimeter scale lithium ion polymer microbatteries for wireless sensors. In: *Sixth international workshop on micro and nanotechnology for power generation and energy conversion applications (PowerMEMS 2006)*, Berkeley, CA.

Huang, D., Liao, F., Molesa, S., Redinger, D., & Subramanian, V. (2003). Plastic-compatible low-resistance printable gold nanoparticle conductors for flexible electronics. *Journal of the Electrochemical Society, 150*(7), G412–G417.

Ko, S. H., Park, I., Pan, H., Grigoropoulos, C. P., Pisano, A. P., Luscombe, C. K., et al (2007). Direct nanoimprinting of metal nanoparticles for nanoscale electronics fabrication. *Nano Letters, 7*, 1869–1877.

Ko, S. H., Park, I., Pan, H., Misra, N., Rogers, M. S., Grigoropoulos, C. P., et al (2008). ZnO nanowire network transistor fabrication by low temperature, all inorganic nanoparticle solution process. *Applied Physics Letters, 92*, 154102.

Maier, S. A., & Atwater, H. A. (2005). Plasmonics: Localization and guiding of electromagnetic energy in metal/dielectric structures. *Journal of Applied Physics, 98*, 01110.

Nakanishi, H., Bishop, K. J. M., Kowalczyk, B., Nitzan, A., Weiss, E. A., Tretiakov, K. V., et al (2009). Photoconductance and inverse photoconductance in thin films of functionalized metal nanoparticles. *Nature, 2009*(460), 371–375.

Park, J.-U., Hardy, M., Kang, S. J., Barton, K., Adair, K., Mukhopadhyay, D. K., et al (2007). High-resolution electrohydrodynamic jet printing. *Nature Materials, 6*, 782–789.

Park, I., Ko, S. H., Pan, H., Grigoropoulos, C. P., Pisano, A. P., Frechet, J. M. J., et al (2008). Nanoscale patterning and electronics on flexible substrate by direct nanoimprinting of metallic nanoparticles. *Advanced Materials, 20*, 489.

Ridley, B. A., Nivi, B., & Jacobson, J. M. (1999). All-inorganic field effect transistors fabricated by printing. *Science, 286*, 746–749.

Samarasinghe, S. R., Pastoriza-Santos, I., Edirisinghe, M. J., Reece, M. J., & Liz-Marzan, L. M. (2006). Printing gold nanoparticles with an electrohydrodynamic direct write device. *Gold Bulletin, 39*, 48–53.

Sirringhaus, H., Kawase, T., Friend, R. H., Shimoda, T., Inbasekaran, M., Wu, W., et al (2000). High-resolution inkjet printing of all-polymer transistor circuits. *Science, 290*, 2123–2126.

Wang, J. Z., Zheng, Z. H., Li, H. W., Huck, W. T. S., & Sirringhaus, H. (2004). Dewetting of conducting polymer inkjet droplets on patterned surfaces. *Nature Materials, 3*, 171–176.